Cutoff Conditions in Three-Layer Cylindrical Dielectric Waveguides

AHMAD SAFAAI-JAZI AND GAR LAM YIP, SENIOR MEMBER, IEEE

Abstract—**Exact cutoff expressions for hybrid and circularly symmetric modes in three-layer cylindrical dielectric waveguides are derived. It is analytically established that whenever the refractive index of the outer medium (n_3) is higher than either the refractive index of the core (n_1) or of the inner cladding (n_2), i.e., $n_1>n_3>n_2$ or $n_2>n_3>n_1$, the dominant HE_{11} mode can have a nonzero cutoff frequency. Inequalities relating the permittivities to the ratio of the cladding radius to the core radius, as conditions for the nonzero cutoff of the HE_{11} mode, are determined. The cutoff conditions presented in this paper are also applicable to similar structures used in millimeter-wave communications.**

I. INTRODUCTION

CYLINDRICAL dielectric surface waveguides are becoming increasingly promising in optical communications. Much effort has been devoted to the analysis of surface waveguides in recent years. Among the various important aspects of dielectric waveguides, cutoff conditions play a major role in the design of such structures and the selection of operating frequencies. In certain cases, a three-layer waveguide can be well approximated by a rod for which exact cutoff expressions for all modes are available [1], [2]. A cladded fiber with a large ratio of the cladding radius to the core radius (r_2/r_1) is often modeled by a dielectric rod [3].

There are, however, circumstances to which the dielectric rod approximation either does not apply or is inadequate, especially when the dominant HE_{11} mode is to be analyzed. In such cases as dielectric tube waveguides, cladded and W-type fibers, new kinds of fibers proposed by Kawakami and Nishida [4], in which the ratio r_2/r_1 is not sufficiently large, one has to deal with a three-layer problem. Knowledge of cutoff conditions in the above mentioned structures provides useful information about the number of guided modes and waveguide dimensions.

Cutoffs for a dielectric tube have been derived for modes with $n=0$ and 1 only, n being the azimuthal number [5]. Derivation of cutoff conditions for modes with $n>1$ in a tube and other three-layer dielectric structures are somewhat complicated, mainly because of the hybrid nature of the modes. It appears that the problem of cutoff conditions in three-layer dielectric waveguides has not yet been comprehensively analyzed. More recently, Safaai-Jazi and Yip [6] derived separate characteristic equations for HE and EH modes in two- and three-layer cylindrical dielectric waveguides with discrete refractive index profiles. After obtaining separate characteristic equations for HE and EH modes, the derivation of the corresponding cutoff conditions is no longer a difficult task.

In this paper, exact cutoff expressions for a three-layer dielectric structure with an arbitrarily discrete index profile are presented. This analysis includes cladded fibers, W-type fibers, dielectric tubes with $n_1=n_3$ and tubes in which the core has a lower refractive index than the outer medium ($n_3>n_1$), and vice versa ($n_1>n_3$).

Kawakami and Nishida [4], in their analysis of the HE_{11} mode in a W-type fiber, found that there are situations where this mode has a nonzero cutoff frequency. Our investigation further reveals that besides the W-type fiber, a tube in which $n_2>n_3>n_1$ can also sustain a HE_{11} mode with a nonzero cutoff frequency. More generally, it can be stated that whenever the refractive index of the outer medium n_3 is higher than either the refractive index of the core n_1 or that of the inner cladding n_2, i.e., $n_1>n_3>n_2$ or $n_2>n_3>n_1$, the HE_{11} mode can have a nonzero cutoff. Simple but exact conditions under which this mode exhibits a cutoff are derived. Variations of cutoff frequencies for several lower order modes in various types of waveguides versus the ratio r_2/r_1 are also presented.

The cutoff expressions presented in this paper are also applicable to similar structures used in millimeter-wave communications.

II. FORMULATION OF THE PROBLEM

Let us consider a cylindrical dielectric waveguide composed of three layers as illustrated in Fig. 1. The ith layer is characterized by a permittivity $\epsilon_i=\epsilon_0\epsilon_{ri}$ and a permeability $\mu_i=\mu_0$. Let $n_i=(\epsilon_{ri})^{1/2}$ denote the refractive index of the ith medium. The discrete refractive index profiles to be used in the present analysis are shown in Fig. 2. Fig. 2(a) represents a cladded fiber. A dielectric tube usually has an index profile as in Fig. 2(b), but profiles of Figs. 2(c) and (d) also represent tubular structures. The profile of the refractive index for a W-type fiber is shown in Fig. 2(e).

The characteristic equations of a three-layer dielectric waveguide having any of the index profiles of Fig. 2 are given by (6), (7), and (11) in [6]. Equations (6) and (7) in [6] are for TE and TM modes, respectively, while (11) in [6] represents HE and EH modes. Cutoff conditions are obtained from the characteristic equations in the limit of

Manuscript received December 19, 1977; revised April 4, 1978. This research was supported by the National Research Council.

The authors are with the Department of Electrical Engineering, McGill University, Montreal, P.Q., Canada H3C 3G1.

0018-9480/78/1100-0898$00.75 ©1978 IEEE

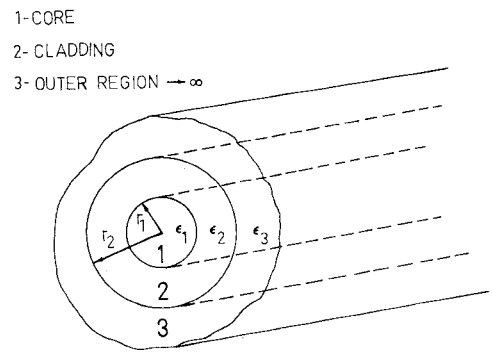

Fig. 1. Geometry of a three-layer cylindrical dielectric structure.

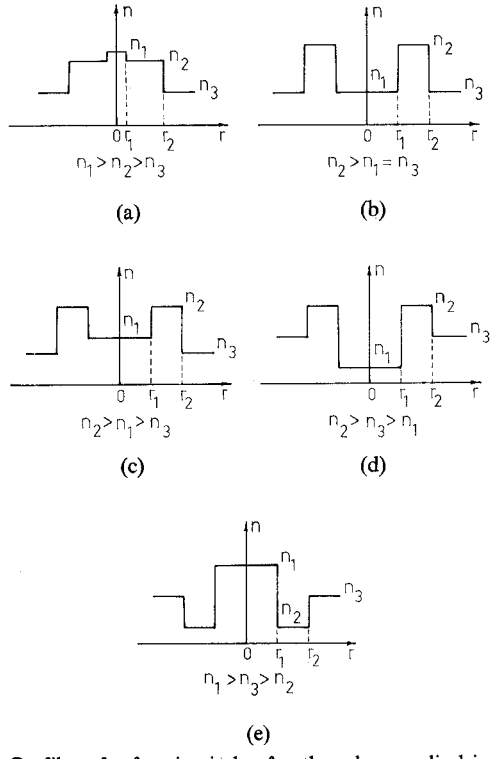

Fig. 2. Profiles of refractive index for three-layer cylindrical dielectric waveguides. (a) For a cladded fiber. (b), (c), and (d) For various types of tubes. (e) For a W-type fiber.

$\bar{\beta}\to n_3$, where $\bar{\beta}=\beta/k_0$ is the normalized propagation constant. Equation (11) in [6] in its present form, however, is not suitable for the derivation of cutoff conditions. Introducing the quantities $\bar{\eta}_i$, $i=1, 2, \cdots, 6$ and $\bar{\Delta}_j$, $j=1, 2, \cdots, 5$, defined in the Appendix, and using the identities (A3) and (A4), (11) in [6] is rewritten as

$$\bar{\eta}_1 = n/\bar{x}^2 + \left\{ -G_2 \pm \left[(G_2')^2 + 4\epsilon_{r1}(\epsilon_{r2}T)^2 \right]^{1/2} \right\} / 2G_1 \quad (1)$$

where G_1, G_2, G_2', and T are given in the Appendix. Equation (1) now has the desired form for the cutoff calculations. Equations (6) and (7) in [6] in terms of the new quantities become

$$\epsilon_{r1}\bar{\eta}_1(\epsilon_{r2}\bar{\Delta}_2 - \epsilon_{r3}\bar{\Delta}_5) - \epsilon_{r2}^2\bar{\Delta}_3 - \epsilon_{r2}\epsilon_{r3}\bar{\Delta}_1\bar{\eta}_6 = 0, \quad \text{for TM modes} \quad (2)$$

$$\bar{\eta}_1(\bar{\Delta}_2 - \bar{\Delta}_5) - \bar{\Delta}_3 - \bar{\Delta}_1\bar{\eta}_6 = 0, \quad \text{for TE modes.} \quad (3)$$

III. Derivation of Cutoff Conditions

Let us first assume that $\epsilon_{r1} \neq \epsilon_{r3}$; then, upon letting $w\to 0$ and using the asymptotic values of $\bar{\eta}_6 = K_{n-1}(w)/wK_n(w)$, given in Table I, we obtain the following results:

$$\bar{\eta}_1 = n/\bar{x}^2 + \left\{ E_2 \pm \sigma\left[(E_2')^2 + 4\epsilon_{r1}\epsilon_{r3}E_3^2 \right]^{1/2} \right\} / 2E_1 \quad (4)$$

where for $n>1$

$$E_1 = -\epsilon_{r1}C_1$$
$$E_2 = (\epsilon_{r1}+\epsilon_{r2})(nC_1/\bar{u}_1^2 - C_2) + \epsilon_{r2}(\epsilon_{r1}+\epsilon_{r3})\bar{\Delta}_4$$
$$E_2' = (\epsilon_{r1}-\epsilon_{r2})(nC_1/\bar{u}_1^2 - C_2) + \epsilon_{r2}(\epsilon_{r1}-\epsilon_{r3})\bar{\Delta}_4$$
$$E_3 = nC_1(1/\bar{x}^2 - 1/\bar{u}_1^2) - \epsilon_{r2}\bar{\Delta}_4$$
$$\sigma = 1$$

with

$$C_1 = (\xi-1)\left[(\epsilon_{r2}+\epsilon_{r3})\bar{\Delta}_2 - \epsilon_{r3}(\xi-1)/(n-1) \right]$$
$$C_2 = (\xi-1)\left[(\epsilon_{r2}+\epsilon_{r3})\bar{\Delta}_3 + \epsilon_{r3}\bar{\Delta}_1/(n-1) \right]$$

and for $n=1$

$$E_1 = \epsilon_{r1}(\xi-1)$$
$$E_2 = -(\epsilon_{r1}+\epsilon_{r2})\left[\bar{\Delta}_1 + (\xi-1)/\bar{u}_1^2 \right]$$
$$E_2' = -(\epsilon_{r1}-\epsilon_{r2})\left[\bar{\Delta}_1 + (\xi-1)/\bar{u}_1^2 \right]$$
$$E_3 = (\xi-1)(1/\bar{x}^2 - 1/\bar{u}_1^2)$$
$$\sigma = \text{sgn}\,(\xi-1).$$

Furthermore, whenever $\epsilon_{r1} > \epsilon_{r3}$, + and − signs in (4) correspond to EH and HE modes, respectively. This case applies to cladded fibers, W-type fibers, and dielectric tubes with refractive index profiles as in Fig. 2(c). For a tube having an index profile as Fig. 2(d), + should be used for HE and − for EH modes.

The HE_{11} mode in most familiar structures such as dielectric rods, dielectric tubes with $\epsilon_{r1}=\epsilon_{r3}$, and cladded fibers is known to have a zero cutoff frequency. In the case of three-layer dielectric waveguides, however, this mode does not always have a zero cutoff. To investigate the cutoff condition of the HE_{11} mode let $\bar{\beta}\to n_3$ and $k_0\to 0$; then with the help of Table I, the characteristic equation (4) in [6] reduces to

$$\frac{\nu_2}{u_1^2} = \left[\frac{\epsilon_{r3}(\epsilon_{r1}+\epsilon_{r2})p(p-1) + 2\epsilon_{r2}\epsilon_{r3}p(\epsilon_{r1}-\epsilon_{r3})/(\epsilon_{r2}-\epsilon_{r3})}{2\epsilon_{r2}(\epsilon_{r1}+\epsilon_{r3}) + (\epsilon_{r1}+\epsilon_{r2})(\epsilon_{r2}+\epsilon_{r3})(p-1)} \right] \cdot \ln(2/\gamma w) \quad (5)$$

where $p=(r_2/r_1)^2$ and $\gamma = 1.781$ is the Euler's constant. For the profiles of Figs. 2(a)–(c), $\nu_2 = +1$, $\epsilon_{r1} \geq \epsilon_{r3}$, and $\epsilon_{r2} > \epsilon_{r3}$; thus as u_1 and w approach zero, (5) is always satisfied, for both sides of it approach $+\infty$, indicating that the HE_{11} mode has a zero cutoff frequency. For a W-type fiber, $\nu_2 = -1$ and $\epsilon_{r1} > \epsilon_{r3} > \epsilon_{r2}$; hence the LHS of (5) $\to -\infty$ while the RHS of it may approach $+\infty$ or $-\infty$. The RHS approaches $-\infty$ whenever the numerator of the square bracketed term is negative, in which case the HE_{11} mode has a zero cutoff. However, if the numerator

is positive, (5) no longer holds, and as a result the HE_{11} mode will have a nonzero cutoff frequency which is obtained from (4) with $-$ sign and $n=1$. Consequently, the condition under which the HE_{11} mode in a W-type fiber exhibits a nonzero cutoff is expressed as follows:

$$\frac{r_2}{r_1} > \left[\frac{(\epsilon_{r3}+\epsilon_{r2})(\epsilon_{r1}-\epsilon_{r2})}{(\epsilon_{r3}-\epsilon_{r2})(\epsilon_{r1}+\epsilon_{r2})} \right]^{1/2}. \tag{6}$$

For a dielectric tube having a refractive index profile as Fig. 2(d), $\nu_2=+1$ and $\epsilon_{r2}>\epsilon_{r3}>\epsilon_{r1}$. In a manner similar to the cutoff analysis of the HE_{11} mode for a W-type fiber, one concludes that this mode has a nonzero cutoff frequency when the condition

$$\frac{r_2}{r_1} < \left[\frac{(\epsilon_{r2}+\epsilon_{r3})(\epsilon_{r2}-\epsilon_{r1})}{(\epsilon_{r2}-\epsilon_{r3})(\epsilon_{r2}+\epsilon_{r1})} \right]^{1/2} \tag{7}$$

is met where the cutoff is obtained from (4) with $+$ sign and $n=1$.

Using (2) and (3) with the help of Table I, cutoff conditions for TE and TM modes are readily obtained.

$$\epsilon_{r1}\bar{\eta}_1(\xi-1)+\epsilon_{r2}\bar{\Delta}_1=0, \qquad \text{for TM modes} \tag{8}$$

$$\bar{\eta}_1(\xi-1)+\bar{\Delta}_1=0, \qquad \text{for TE modes.} \tag{9}$$

It can be verified that in the limiting case of $r_2/r_1\to 1$, the cutoffs for a cladded fiber reduce to those for a dielectric rod.

The cutoff conditions for a tube in which $\epsilon_{r1}=\epsilon_{r3}$ can be obtained from (4), (8), and (9) by letting $x\to 0$ and using $-$ sign for EH and $+$ for HE modes in (4). It should be noted that ν_1 is always -1 for this waveguide. Upon letting $x\to 0$ and using Table I, the following results are derived. For $n>1$,

$$(\epsilon_{r1}+\epsilon_{r2})(2nC_1/\bar{u}_1^2-C_2)+4\epsilon_{r1}\epsilon_{r2}\bar{\Delta}_4-\epsilon_{r1}C_1/2=0. \tag{10}$$

Equation (10) gives cutoffs for HE modes whenever $C_1>0$ and cutoffs for EH modes when $C_1<0$. $C_1=0$ never occurs, because if C_1 becomes zero (10) reduces to

$$\left[\frac{2(\epsilon_{r2}-\epsilon_{r1})}{\pi u_1 u_2 J_n(u_1) Y_n(u_2)} \right]^2 = 0$$

which is not possible. Cutoff conditions for the cases $n=0$ and 1 had been obtained before [5] and thus are not given here.

IV. Core Mode Cutoffs for Cladded Fibers

In cladded fibers $\bar{\beta}$ varies from n_3 to n_1 for guided modes. The frequencies at which $\bar{\beta}=n_2$ have been referred to as core-mode cutoffs [3], although the concept of cutoff, strictly speaking, does not really apply to them. In other words, if the core-mode cutoff frequency of a certain mode is higher than the operating frequency, that mode might still be present as a cladding mode, although weakly confined to the core. For efficient signal transmission, core modes should be used. Hence, the role of the core-mode cutoffs dominates over that of the cladding-mode cutoffs (actual cutoffs, $\bar{\beta}=n_3$). In deriving the core-mode cutoffs, one may let $\bar{\beta}$ approach n_2 in the core-mode region $(n_1>\bar{\beta}>n_2)$ or in the cladding-mode region $(n_2>\bar{\beta}>n_3)$. The continuity of the dispersion characteristics at $\bar{\beta}=n_2$ ensures that the results do not depend on how $\bar{\beta}$ approaches n_2.

TABLE I
Small-Argument Approximations

n	$\frac{J_{n-1}(t)}{tJ_n(t)}$	$\frac{Y_{n-1}(t)}{tY_n(t)}$	$\frac{I_{n-1}(t)}{tI_n(t)}$	$\frac{K_{n-1}(t)}{tK_n(t)}$	$\frac{J_n(ct)Y_n(t)}{J_n(t)Y_n(ct)}$
$n\geq 2$	$\frac{2n}{t^2}-\frac{1}{2(n+1)}$	$\frac{1}{2(n-1)}$	$-\frac{2n}{t^2}-\frac{1}{2(n+1)}$	$\frac{1}{2(n-1)}$	$(c)^{2n}$
$n=1$	$-\frac{2}{t^2}-\frac{1}{4}$	$\ln(\frac{2}{\gamma t})$	$-\frac{2}{t^2}-\frac{1}{4}$	$\ln(\frac{2}{\gamma t})$	$(c)^2$
$n=0$	$-\frac{1}{2}$	$\frac{1}{t^2\ln(\frac{\gamma t}{2})}$	$\frac{1}{2}$	$\frac{-1}{t^2\ln(\gamma t/2)}$	$\frac{1}{c}$

After letting $\bar{\beta}\to n_2$ or equivalently letting u_1 and $u_2\to 0$ and using the small-argument approximations given in Table I, (1) becomes

$$\bar{\eta}_1 = n/x^2 + \left\{ \bar{G}_2 \pm \left[(\bar{G}_2')^2 + 4\epsilon_{r1}\epsilon_{r2}\bar{G}_3^2 \right]^{1/2} \right\} / 2\bar{G}_1 \tag{11}$$

where

$$\bar{G}_1 = 4\epsilon_{r1}\epsilon_{r2}q/p$$

$$\bar{G}_2 = H, \qquad \text{with the upper sign}$$

$$\bar{G}_2' = H, \qquad \text{with the lower sign}$$

$$\bar{G}_3 = 4n\epsilon_{r2}q/px^2 + 2nq[2\epsilon_{r2}+(\epsilon_{r2}+\epsilon_{r3})(q-1)]/w^2 + (\epsilon_{r2}+\epsilon_{r3})(q^2-1)\bar{\eta}_6 - 2\epsilon_{r2}S + \epsilon_{r2}(q-1/p)q/(n+1)$$

$$H = 2q(n/w^2+\bar{\eta}_6)[2\epsilon_{r2}(\epsilon_{r1}\pm\epsilon_{r3})+(\epsilon_{r2}+\epsilon_{r3})(\epsilon_{r1}\pm\epsilon_{r2}) \cdot (q-1)] + 2\epsilon_{r2}(\epsilon_{r1}\pm\epsilon_{r2})S - (\epsilon_{r1}\pm\epsilon_{r2})(\epsilon_{r2}+\epsilon_{r3})(q^2-1)\bar{\eta}_6 + \epsilon_{r2}(\epsilon_{r1}\pm\epsilon_{r2})q(q-1/p)/(n+1)$$

with $q=(r_2/r_1)^{2n}$, $p=(r_2/r_1)^2$, and $S=\ln(r_2/r_1)$ for $n=1$ and $S=[p^{(n-1)}-1]/2(n-1)$ for $n>1$. Also $+$ and $-$ in (11) correspond to EH and HE modes, respectively. When $n=0$, from (2) and (3) with the help of Table I,

$$\epsilon_{r2}(p^{1/2}-1)/2+\epsilon_{r3}p^{1/2}\bar{\eta}_6-\epsilon_{r1}\bar{\eta}_1=0, \qquad \text{for TM modes} \tag{12}$$

$$(p^{1/2}-1)/2+p^{1/2}\bar{\eta}_6-\bar{\eta}_1=0, \qquad \text{for TE modes.} \tag{13}$$

V. Numerical Results

Cutoff values for several lower order modes are obtained by numerically solving the cutoff equations derived in Sections III–V. Table II summarizes the typical values of permittivities used in cutoff computations. Plots of cutoff frequencies versus the ratio r_2/r_1 are presented. The notation V_c representing the normalized cutoff frequency has the following definition:

$$V_c = \frac{2\pi r_1}{\lambda_c}\sqrt{|\epsilon_{r1}-\epsilon_{r2}|}\,.$$

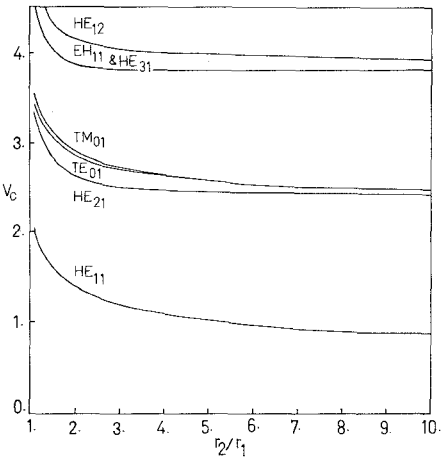

Fig. 3. Coré-mode cutoff variations for the HE_{11}, HE_{21}, TE_{01}, TM_{01}, EH_{11}, HE_{31}, and HE_{12} modes versus r_2/r_1 in a cladded fiber with $\epsilon_{r1}=2.341$, $\epsilon_{r2}=2.250$, and $\epsilon_{r3}=1.000$.

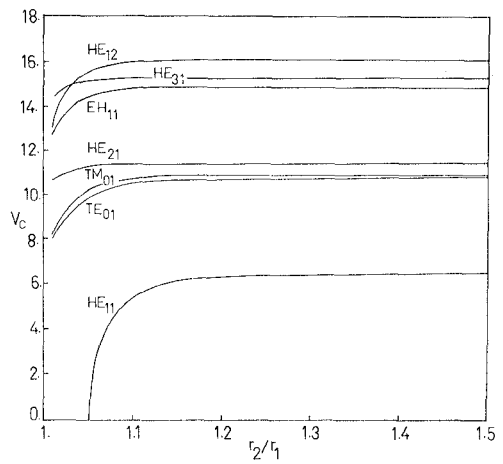

Fig. 4. Cutoff variations for the HE_{11}, TE_{01}, TM_{01}, HE_{21}, EH_{11}, HE_{31}, and HE_{12} modes versus r_2/r_1 in a W-type fiber with $\epsilon_{r1}=2.250$, $\epsilon_{r2}=1.822$, and $\epsilon_{r3}=2.205$.

TABLE II
PERMITTIVITIES FOR THREE-LAYER DIELECTRIC WAVEGUIDES

permittivities	cladded fiber	W-type fiber	tube $\epsilon_{r1}=\epsilon_{r3}$	tube $\epsilon_{r3}>\epsilon_{r1}$	tube $\epsilon_{r1}>\epsilon_{r3}$
ϵ_{r1}	2.341	2.250	1.000	1.000	1.210
ϵ_{r2}	2.250	1.822	2.250	2.250	2.250
ϵ_{r3}	1.000	2.205 *	1.000	2.205 *	1.000

Actually, $n_3=1.4849$ has been used in the computations.

Fig. 3 shows the core-mode cutoffs for a cladded fiber. It is observed that when $r_2/r_1 \gg 1$, the cutoff values of all modes with the exception of the HE_{11} mode are very close to their respective values in a dielectric rod with $\epsilon_{r1}=2.341$ and $\epsilon_{r2}=2.250$ [3], whereas for $r_2/r_1<2.5$ they considerably differ from the cutoffs in the corresponding rod approximation. This indicates that the dielectric rod approximation of a cladded fiber does not allow the accurate evaluation of cutoffs for the HE_{11} mode in particular and for the lower order modes, when r_2/r_1 is not much larger than unity, in general.

Fig. 4 illustrates the variation of cutoff frequencies for several modes in a W-type fiber. From (6) it is expected that the HE_{11} mode should have a nonzero cutoff when r_2/r_1 becomes greater than 1.0512. As Fig. 4 shows, the cutoff behavior of this mode perfectly agrees with the inequality (6). For $r_2/r_1>1.2$ there are virtually no or little variations in the cutoffs of all modes, indicating that the W-type fiber under investigation can be well-approximated by a rod with permittivities the same as those of the core and the inner cladding of the fiber [4], [7]. Let us define

$$\Delta(k_c r_1)=(k_c r_1)_{TE_{01}}-(k_c r_1)_{HE_{11}}$$

as the bandwidth of the HE_{11} mode, where $k_c=2\pi/\lambda_c$. For the cladded fiber of Fig. 3 at $r_2/r_1=5$, $\Delta(k_c r_1)=5.13$, whereas for the W-type fiber at $r_2/r_1=1.3$, $\Delta(k_c r_1)=6.64$. Hence, a W-type fiber provides a wider bandwidth than a cladded fiber, making it more practicable for single-mode operation. A similar shifting effect of cutoff frequencies is observed for other modes too. It should be understood, however, that the overall advantage of one structure over another cannot be judged by their cutoff behaviors alone. Other important aspects such as dispersion and radiation loss also must be taken into account.

TABLE III
CUTOFF V_c VALUES FOR CLADDED FIBER AT $r_2/r_1=5$ AND FOR W-TYPE FIBER AT $r_2/r_1=1.3$

cladding mode cutoffs		core mode cutoffs		cutoffs for W fiber	
mode	cutoff value	mode	cutoff value	mode	cutoff value
HE_{11}	0.0000	HE_{11}	1.0328	HE_{11}	6.4468
TM_{01}	0.1293	HE_{21}	2.4543	TE_{01}	10.7958
TE_{01}	0.1297	TE_{01}	2.5806	TM_{01}	10.9731
HE_{21}	0.1508	TM_{01}	2.5915	HE_{21}	11.4919
EH_{11}	0.2056	EH_{11}	3.8333	EH_{11}	14.8992
HE_{12}	0.2067	HE_{31}	3.8541	HE_{31}	15.3625
HE_{31}	0.2311	HE_{12}	3.9914	HE_{12}	16.1066
EH_{21}	0.2765	EH_{21}	5.1356	EH_{21}	18.3636
TM_{02}	0.2961	HE_{41}	5.1589	HE_{41}	19.1133
TE_{02}	0.2974	HE_{22}	5.5424	TE_{02}	20.6179
HE_{41}	0.3030	TE_{02}	5.6062	TM_{02}	20.7976
HE_{22}	0.3089	TM_{02}	5.6108	HE_{22}	21.3548
EH_{31}	0.3442	EH_{31}	6.3801	EH_{31}	22.2032
HE_{51}	0.3714	HE_{51}	6.4050	HE_{51}	22.7824
EH_{12}	0.3757	EH_{12}	7.0164	EH_{12}	25.0172

The cladding-mode cutoffs of a cladded fiber do not convey much practical significance. They are generally much lower than the core mode cutoffs. Table III summarizes the cutoff V_c values of the 15 lower order modes. A comparison of the cladding and the core-mode cutoff values shows that even in the single-mode operation a large number of cladding modes can get excited.

Cutoff variations for tubular structures are shown in Figs. 5–7. Fig. 5 illustrates the cutoffs for a tube in which $\epsilon_{r1}=\epsilon_{r3}$, while Figs. 6 and 7 show the cutoffs for tubes with $\epsilon_{r1}>\epsilon_{r3}$ and $\epsilon_{r3}>\epsilon_{r1}$, respectively. The cutoff frequency of the HE_{11} mode in tubes with $\epsilon_{r1}\geq\epsilon_{r3}$ is always zero, whereas for the case $\epsilon_{r3}>\epsilon_{r1}$ with the help of inequality (7), this mode is expected to have a nonzero cutoff as long as r_2/r_1 remains less than 6.1706. The computed results for the HE_{11} mode given in Fig. 7 verify the correctness of (7). A comparison of Figs. 5–7 shows that the cutoff values in the $\epsilon_{r1}>\epsilon_{r3}$ case are somewhat lower than the

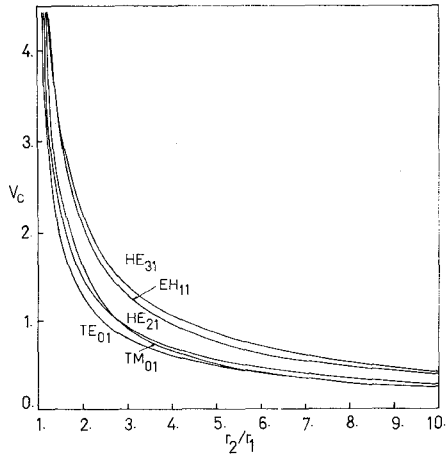

Fig. 5. Cutoff variations for the TE_{01}, TM_{01}, HE_{21}, EH_{11}, and HE_{31} modes versus r_2/r_1 in a tube with $\epsilon_{r1}=\epsilon_{r3}=1.000$ and $\epsilon_{r2}=2.250$.

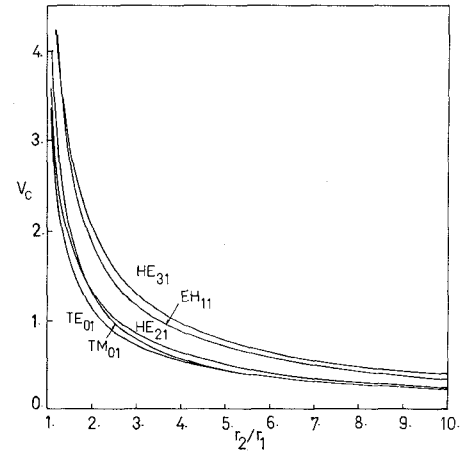

Fig. 6. Cutoff variations for the TE_{01}, TM_{01}, HE_{21}, EH_{11}, and HE_{31} modes versus r_2/r_1 in a tube with $\epsilon_{r1}=1.210$, $\epsilon_{r2}=2.250$, and $\epsilon_{r3}=1.000$.

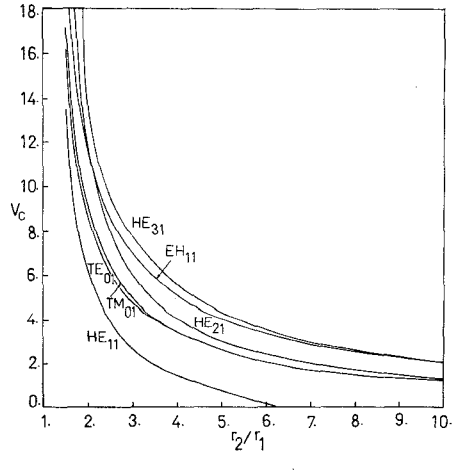

Fig. 7. Cutoff variations for the HE_{11}, TE_{01}, TM_{01}, HE_{21}, EH_{11}, and HE_{31} modes versus r_2/r_1 in a tube with $\epsilon_{r1}=1.000$, $\epsilon_{r2}=2.250$, and $\epsilon_{r3}=2.205$.

corresponding values in the $\epsilon_{r1}=\epsilon_{r3}$ case which in turn are much lower than those of the $\epsilon_{r3}>\epsilon_{r1}$ case: hence a tube in which $\epsilon_{r3}>\epsilon_{r1}$ is capable of providing a much larger bandwidth, a clear advantage for single-mode operation. The

TABLE IV
CUTOFF V_c VALUES FOR TUBES AT $r_2/r_1=3$

$\epsilon_{r1}>\epsilon_{r3}$		$\epsilon_{r1}=\epsilon_{r3}$		$\epsilon_{r1}<\epsilon_{r3}$	
mode	cutoff value	mode	cutoff value	mode	cutoff value
HE_{11}	0.0000	HE_{11}	0.0000	HE_{11}	2.6753
TE_{01}	0.7397	TE_{01}	0.8127	TE_{01}	4.7376
TM_{01}	0.7973	TM_{01}	0.8892	TM_{01}	4.9164
HE_{21}	0.8744	HE_{21}	0.9468	HE_{21}	6.0380
EH_{11}	1.1852	EH_{11}	1.3037	EH_{11}	6.9540
HE_{31}	1.3194	HE_{31}	1.4344	HE_{31}	7.7818
HE_{12}	1.4182	HE_{12}	1.6356	EH_{21}	9.0246
EH_{21}	1.5326	EH_{21}	1.7282	HE_{41}	9.7178
HE_{41}	1.7172	HE_{41}	1.8740	EH_{31}	11.2262
TE_{02}	1.8170	TE_{02}	2.0157	HE_{51}	11.7335
HE_{22}	1.8461	HE_{22}	2.0795	HE_{12}	11.7496
EH_{31}	1.9430	EH_{31}	2.1332	TE_{02}	12.3874
TM_{02}	1.9569	TM_{02}	2.2089	TM_{02}	12.6433
HE_{51}	2.0967	HE_{51}	2.2925	HE_{22}	13.2320
EH_{12}	2.2725	EH_{12}	2.5189	EH_{41}	13.3383

cutoff values for the 15 lower order modes are given in Table IV.

The numerical results presented above also reflect the effects of the variations of ϵ_{r1} and ϵ_{r2} on cutoffs, since the transformation of one structure into another may be attributed to the changes in ϵ_{r1} and ϵ_{r2}. It is evident that an increase in ϵ_{r1} or ϵ_{r2} results in a decrease in cutoff frequencies. Finally, it is emphasized that the conditions for the single-mode operation of a W-type fiber and of a tube depend on the cutoff frequencies of both the HE_{11} and the next higher order mode (TE_{01}, TM_{01}, or HE_{21}), whereas the single-mode condition of a step- or a graded-index optical fiber is determined by only the cutoff frequency of the TM_{01} mode.

VI. Conclusions

Cutoff conditions for all modes in three-layer cylindrical dielectric waveguides with arbitrarily discrete refractive index profiles have been derived. In W-type fibers and tubes in which $\epsilon_{r2}>\epsilon_{r3}>\epsilon_{r1}$, the dominant HE_{11} mode may exhibit a nonzero cutoff. Conditions under which this mode has a nonzero cutoff have been derived. Among the tubular structures, a tube with $\epsilon_{r3}>\epsilon_{r1}$, and among all three-layer structures with comparable parameters, the W-type fiber provides the widest bandwidth for a single-mode operation. Cutoff variations for several lower order modes versus the ratio r_2/r_1 and cutoff values for the 15 lower order modes in all cases have also been presented.

VII. Appendix

1) Definitions of $\bar{\eta}_i$ where $i=1, 2, \cdots, 6$:

$$\bar{\eta}_1=\nu_1\frac{Z_{m1}(x)}{xZ_{n1}(x)} \qquad \bar{\eta}_2=\nu_2\frac{Z_{m2}(u_1)}{u_1Z_{n1}(u_1)} \qquad \bar{\eta}_3=\frac{Z_{m3}(u_1)}{u_1Z_{n3}(u_1)}$$

$$\bar{\eta}_4=\nu_2\frac{Z_{m2}(u_2)}{u_2Z_{n2}(u_2)} \qquad \bar{\eta}_5=\frac{Z_{m3}(u_2)}{u_2Z_{n3}(u_2)} \qquad \bar{\eta}_6=\frac{Z_{m4}(w)}{wZ_{n4}(w)} \tag{A1}$$

where $m=n-1$, $x=k_1r_1$, $u_1=k_2r_1$, $u_2=k_2r_2$, and $w=k_3r_2$, with

$$k_i=k_0\sqrt{\nu_i(\epsilon_{ri}-\bar{\beta}^2)}\,, \qquad i=1,2,3$$

TABLE V
DEFINITIONS OF FUNCTIONS Z_n

Z_{n1}		Z_{n2}		Z_{n3}		Z_{n4}
$\nu_1=1$	$\nu_1=-1$	$\nu_2=1$	$\nu_2=-1$	$\nu_2=1$	$\nu_2=-1$	$\nu_3=-1$
J_n	I_n	J_n	I_n	Y_n	K_n	K_n

and

$$\nu_i=\begin{cases} 1, & \epsilon_{ri}>\bar{\beta}^2 \\ -1, & \epsilon_{ri}<\bar{\beta}^2 \end{cases}$$

and the functions Z_n are summarized in Table V. In Table V, J_n and Y_n are the Bessel functions and I_n and K_n are the modified Hankel functions of order n.

2) Definitions of $\bar{\Delta}_j$ where $j=1, 2, \cdots, 5$:

$$\bar{\Delta}_1=\bar{\eta}_2-\xi\bar{\eta}_3 \quad \bar{\Delta}_2=\xi\bar{\eta}_4-\bar{\eta}_5$$
$$\bar{\Delta}_3=\xi\bar{\eta}_3\bar{\eta}_4-\bar{\eta}_2\bar{\eta}_5 \quad \bar{\Delta}_4=\xi(\bar{\eta}_2-\bar{\eta}_3)(\bar{\eta}_4-\bar{\eta}_5)$$
$$\bar{\Delta}_5=(\xi-1)\bar{\eta}_6 \tag{A2}$$

where

$$\xi=\frac{Z_{n2}(u_2)Z_{n3}(u_1)}{Z_{n2}(u_1)Z_{n3}(u_2)}.$$

3) The Bessel- and modified Hankel-function identities:

$$tB_n'(t)=tB_{n-1}(t)-nB_n(t) \tag{A3}$$

where B_n can be J_n, Y_n, or I_n. Also,

$$tK_n'(t)=-tK_{n-1}(t)-nK_n(t). \tag{A4}$$

4) Expressions for G_1, G_2, G_2' and T:

$$G_1=\epsilon_{r1}\epsilon_{r2}H_1$$
$G_2=H_2$, with the upper sign
$G_2'=H_2$, with the lower sign

$$T^2=\left\{n\bar{\beta}\left[\left(1/\bar{x}^2-1/\bar{u}_1^2\right)H_1+\epsilon_{r2}\left(1/\bar{u}_2^2-1/\bar{w}^2\right)\bar{\Delta}_4\right]\right\}^2$$
$$=n^2\left[\left(\epsilon_{r1}/\bar{x}^2-\epsilon_{r2}/\bar{u}_1^2\right)H_1+\epsilon_{r2}\left(\epsilon_{r2}/\bar{u}_2^2-\epsilon_{r3}/\bar{w}^2\right)\bar{\Delta}_4\right]$$
$$\cdot\left[\left(1/\bar{x}^2-1/\bar{u}_1^2\right)H_1+\epsilon_{r2}\left(1/\bar{u}_2^2-1/\bar{w}^2\right)\bar{\Delta}_4\right]$$
$$H_1=\left(\epsilon_{r2}\bar{\Delta}_2-\epsilon_{r3}\bar{\Delta}_5\right)\left(\bar{\Delta}_2-\bar{\Delta}_5\right)-n(\xi-1)\left\{\left[2\epsilon_{r2}\bar{\Delta}_2\right.\right.$$
$$\left.-\left(\epsilon_{r2}+\epsilon_{r3}\right)\bar{\Delta}_5\right]/\bar{u}_2^2-\left[\left(\epsilon_{r2}+\epsilon_{r3}\right)\bar{\Delta}_2-2\epsilon_{r3}\bar{\Delta}_5\right]/\bar{w}^2\Big\}$$
$$H_2=\epsilon_{r2}\Big\{n\left(\epsilon_{r1}\pm\epsilon_{r2}\right)H_1/\bar{u}_1^2-n\epsilon_{r2}\bar{\Delta}_4\left[\left(\epsilon_{r1}\pm\epsilon_{r2}\right)/\bar{u}_2^2\right.$$
$$\left.-\left(\epsilon_{r1}\pm\epsilon_{r3}\right)/\bar{w}^2\right]+n\left(\epsilon_{r1}\pm\epsilon_{r2}\right)(\xi-1)\left[\bar{\Delta}_3\left(2\epsilon_{r2}/\bar{u}_2^2\right.\right.$$
$$\left.-\left(\epsilon_{r2}+\epsilon_{r3}\right)/\bar{w}^2\right)+\bar{\Delta}_1\bar{\eta}_6\left(\left(\epsilon_{r2}+\epsilon_{r3}\right)/\bar{u}_2^2-2\epsilon_{r3}/\bar{w}^2\right)\Big]$$
$$-\epsilon_{r1}\left(\epsilon_{r2}\bar{\Delta}_2-\epsilon_{r3}\bar{\Delta}_5\right)\left(\bar{\Delta}_3+\bar{\Delta}_1\bar{\eta}_6\right)\mp\epsilon_{r2}\left(\bar{\Delta}_2-\bar{\Delta}_5\right)$$
$$\cdot\left(\epsilon_{r2}\bar{\Delta}_3+\epsilon_{r3}\bar{\Delta}_1\bar{\eta}_6\right)\Big\}$$

where $\bar{x}^2=\nu_1x^2$, $\bar{u}_1^2=\nu_2u_1^2$, $\bar{u}_2^2=\nu_2u_2^2$, and $\bar{w}^2=\nu_3w^2$.

5) Small-argument approximations: Table I summarizes the asymptotic expressions for various terms with small arguments.

REFERENCES

[1] E. Snitzer, "Cylindrical dielectric waveguide modes," *J. Opt. Soc. Am.*, vol. 51, pp. 491–498, May 1961.
[2] D. Marcuse, *Light Transmission Optics*. Princeton, NJ: Van Nostrand-Reinhold, 1972.
[3] P. J. B. Clarricoats and K. B. Chan, "Propagation behaviour of cylindrical dielectric-rod waveguides," *Proc. Inst. Elec. Eng.*, vol. 120, no. 11, pp 1371–1378, Nov. 1973.
[4] S. Kawakami and S. Nishida, "Characteristics of a doubly-clad optical fiber with a low-index inner cladding," *IEEE J. Quantum Electron.*, vol. QE-10, pp. 879–887, Dec. 1974.
[5] M. M. Z. Kharadly and J. E. Lewis, "Properties of dielectric tube waveguides," *Proc. Inst. Elec. Eng.*, vol. 116, no. 2, pp. 214–224, Feb. 1969.
[6] A. Safaai-Jazi and G. L. Yip, "Classification of hybrid modes in cylindrical dielectric optical waveguides," *Radio Sci. (Special Issue on Fiber and Integrated Optics)*, vol. 12, no. 4, pp. 603–609, July–Aug. 1977.
[7] S. Kawakami and S. Nishida, "Perturbation theory of a doubly-clad fiber with a low-index inner cladding," *IEEE J. Quantum Electron.*, vol. QE-11, Apr. 1975.